Asian Journal of Chemistry; Vol. 37, No. 9 (2025), 2232-2236
ASIAN JOURNAL OF CHEMISTRY
https://doi.org/10.14233/ajchem.2025.33908

Corrosion and Surface Modification of Hybridized Seashell Composite on AA6063 Alloy for Advance Application

OJO S.I. FAYOMI[1,2,3,*], OTITOLAYE A. AJIBOLA[1,4], HO SOON MIN[2] and KUNLE M. OLUWASEGUN[5]

[1]Department of Mechanical Engineering, Bells University of Technology, Ota, Nigeria
[2]Faculty of Health and Life Sciences, INTI International University, Putra Nilai, 71800, Negeri Sembilan, Malaysia
[3]Department of Mechanical Engineering Science, University of Johannesburg, Auckland Pack, Kingsway Campus, Johannesburg, South Africa
[4]Department of Foundary Engineering, Kogi State Polytechnic, Lokoja, Kogi State, Nigeria
[5]Department of Mechanical and Manufacturing Engineering, University of Manitoba, Winnipeg, Manitoba, Canada

*Corresponding author: E-mail: osfayomi@bellsuniversity.edu.ng

Received: 21 April 2025 *Accepted*: 9 August 2025 *Published online*: 30 August 2025 AJC-22103

This study focuses on utilizing abundantly available seashell ash by dispersing it in AA6063 alloy to form composites. A new aluminium metal matrix composite was developed by reinforcing AA 6063 alloy with particles of seashell ash as reinforcement materials in varying percentages (0, 10, 20, 30, 40 wt.%). The samples were prepared by using the stir casting method. The microstructural characterizations were carried out using optical microscopy and the scanning electron microscope (SEM), revealing particle shape and size descriptions for the composite microstructural features. The results indicate that the composite materials exhibit relatively larger and more uniformly distributed grain sizes compared to the base material. The outcomes demonstrate a significant improvement in the tensile strength and hardness of the composites, accompanied by a decrease in corrosion rates. The best samples display a 90.95% increase in tensile strength, a 38.01% increase in hardness and a 71.5% decrease in corrosion rate in an HCl environment, along with a 46.7% decrease in a NaCl environment. Furthermore, there is a 207.7% increase in impact strength in the sample reinforced with 20 wt.% of seashell ash. Overall, the AA-SS composite with 20% wt. seashell ash exhibits the most favourable properties, featuring a 90.95% increase in tensile strength, a 38.01% increase in hardness and a lower corrosion rate when compared to the control sample.

Keywords: Aluminium, Seashell composite, Reinforcement, Casting, Defects.

INTRODUCTION

The engineering materials, particularly those used in the automotive and aviation industries, demand materials that are stronger, lighter and most importantly, less expensive [1]. The desire for these materials stems from the need to produce light weight structural parts and engine components with a high strength-to-weight ratio [2]. This has the potential to substantially decrease the excessive use of fuel and the resulting excess CO_2 emissions [3]. The use of lightweight materials in internal combustion (IC) engines enhances fuel efficiency by reducing overall vehicle weight and improving engine performance [4]. Good resistance to corrosion, mechanical, physical and wear properties are required for the mechanical strength of compact engineering materials in the industrial sector [5]. However, none of these properties have been reported in naturally occurring or monolithic engineering materials or metals [6,7].

According to Fayomi *et al*. [8], the consistent use of aluminium alloy is reasonable because of its excellent isotropic characteristics, lower density, average cost effectiveness and better corrosion response. Although several aluminium alloys exist, however, 6063 are significantly used due to reduction to stress initiation, pronounced weldability and sustained strengthening behaviours during structural application [9]. No doubt, interfacial propagation arises as results of proper modification and passive oxidation of the injected particulate into the aluminum melt against potential solid crack or failure [10]. In practice, there is reduction in instability, shock and deterioration of solid structure due to nano phase and composite particle diffusion such as SiC, Al_2O_3 and ZrB_2 due to their characteristics tendency to provide solid bound. Again, studies shows

that liquid metallurgy process involves volume fraction and size concentration which are major consideration in alloy development framework [11].

Amid the array of discrete dispersions employed, melon husk ash emerges as a particularly economical and lightweight reinforcement, conveniently obtainable in substantial volumes as a residual byproduct [12]. As a result, composites that incorporate organic ash for reinforcement hold promise in circumventing financial constraints and finding diverse utility. The current study centres on the pragmatic utilization of readily accessible seashell ash, dispersed within AA6063 alloy, to craft composite materials. Aluminium is widely used in engineering for structural purposes due to its lightweight, durability, non-corrosive nature, machinability and good heat and electrical conductivity [13]. However, in some applications, its functionality is limited and researches have been conducted to improve its properties. Therefore, there is a need to investigate the effect of seashell powder particulates on the microstructure and mechanical properties of Al6063. The aim of this study is to develop and characterize a new AA6063 reinforced seashell alloy for service life improvement.

EXPERIMENTAL

The composite development involved the utilization of AA6063 aluminium alloy as the matrix material. This aluminium alloy, renowned for its favourable attributes such as excellent corrosive resistance, high workability and exceptional weldability, was selected to form the foundation of the composite. To initiate the fabrication process, the substrate material was acquired from a reliable metal market located in Ota, Nigeria. Before incorporation into the composite, the substrate material underwent a series of preparatory steps to ensure its quality and suitability. The substrate was meticulously descaled to eliminate any surface impurities that could potentially impact the overall performance of the composite. Furthermore, thorough cleaning procedures were applied to get a pristine surface, which is free from contaminants. To delve further into the characteristics and composition of the substrate material, the aluminium alloy and the sea shell particulate were examined using spectrometer analyzer and X-ray fluorescence (XRF) analysis, respectively. The chemical compositions are presented in Table-1 and Table-2 represents the alloy development design of experiment and fabrication ratio.

TABLE-1
ELEMENTAL AND CHEMICAL COMPOSITIONS OF MATERIALS USED

AA6063		Seashell ash	
Element	Percentage	Chemical composition	Percentage
Si	1.20	CaO	52.34
Cu	5.00	SiO_2	4.55
Fe	0.70	Al_2O_3	0.06
Mn	0.12	Fe_2O_3	0.20
Zn	0.25	SO_3	0.47
Ti	0.15	Na_2O	0.25
Mg	0.80	K_2O	0.23
Cr	0.10	MgO	0.32
Al	Bal.	Cl	0.1038
–	–	Loss on ignition	41.252

TABLE-2
CHARGE CALCULATION OF THE COMPOSITE

Sample	AA6063 weight (g)	Weight of AA-SS (g)	Total wt. (%)
Control	100	–	100
AA-10SS	90	10	100
AA-20SS	80	20	100
AA-30SS	70	30	100
AA-40SS	60	40	100

Preparation of seashell composite: The seashells were acquired from one of the beaches in Lagos, Nigeria. In order to get the shells ready, they were combined with a 2:1 combination of water and acetone to eliminate any potential impurities. The seashells were then soaked in NaCl treated warm water to further eliminate inorganic contaminants. The already washed seashells were then sun dried for 96 h to remove residual moisture content. The seashells were first crushed and then a high ball milling machine (MQ7501060) was used to grind them into a fine powder. To make sure that the milled sample produced excellent-quality powder, it was sieved through a 60 μm mesh. Each batch of the prepared seashell powder weighed 500 g and then added to the crucible for calcination. The seashell ash was carefully sieved using different sizes of mechanical sieve apparatus, from 100 μm to 45 μm, which were used to achieve the desired particle size.

RESULTS AND DISCUSSION

Microstructure characterization of the composites: The microstructural attributes of the respective reinforcements based on particle volume ratio. From the control sample, as illustrated in Fig. 1a, an intriguing observation shows microvoids on the metal surface, potentially acting as vulnerable sites prone to attack and instability. The surface composition seems to adopt a nodular configuration, an aspect that could significantly influence the behaviour of material. In Fig. 1b, portraying the AA-10SS sample, a different narrative unfolds with distinct reduction in void presence across the surface. This outcome strongly suggests that the seashell particles have seamlessly integrated within the aluminium matrix which agrees with the other researchers [14-16], achieving a more cohesive and harmonious arrangement. Upon closer inspection, it becomes obvious that little spherical particles decoration larger nodal structures on the aluminum surface. This phenomenon signals an intriguing non-uniform distribution within the phase and along the boundary.

Upon careful inspection of the microstructural response of the alloy (Fig. 1c), the microstructure reveals an arrangement of enhanced refinement and exceptional uniformity. This characteristic pointed to the significant absence of visible voids within the metal lattices as a close loop conditional properties of seashell essential oxides. In other words, the trait signifies a finely tuned composition of mutual covenant bond particulate demonstrating positive recrystallization behaveour within metal matrix. The refined microstructure offers promising implications for the performance of material under varied circumstances, highlighted the potential for enhanced durability and resistance [17].

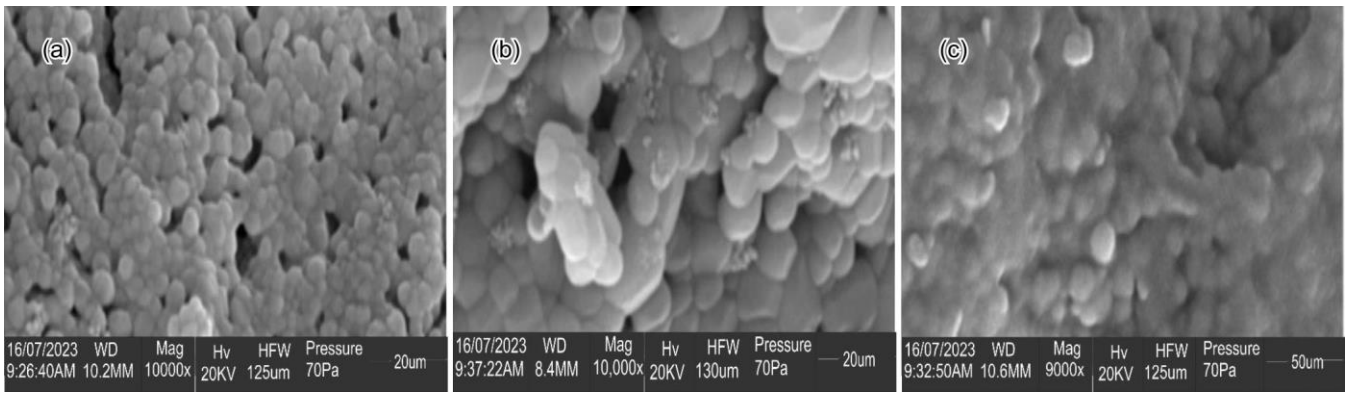

Fig. 1. SEM images of (a) control sample, (b) AA-10SS sample and (c) AA-40SS sample

Electrochemical profile of AA-SS in HCl and NaCl: Fig. 2 illustrates the open circuit potential (OCP) of the developed alloy when exposed to HCl and NaCl. The corrosion potential exhibited a shift towards the positive direction due to the presence of a predominant nanophase component, which effectively contributed to the formation of an extensive protective film against chloride ions over time. It is noteworthy to mention that the presence of particulate dispersed within the aluminium phase is observed to be significantly active to retard possible active surfaces where corrosion ion might have penetrated [18]. Table-3 presents the polarization data and parameters, including corrosion resistance (CR). Furthermore, Fig. 3 illustrates the polarization curves specific to AA-SS in the presence of HCl. Remarkably, the control sample displayes the highest corrosion resistance (CR), elevated corrosion current density (J_{corr}) values and the least polarization resistance (PR). As the reinforcement within the sample increases, a prominent trend unfolds: the CR diminishes, J_{corr} values decrease and PR exhibits an accelerating pattern. This interesting relationship highlights the considerable impact of the SS nanoparticles' integration within the matrix. Notably, this amalgamation of nanoparticles brings about enhanced oxidation and corrosion resistance. This fortification is attributed to the infusion of SS nanoparticles into the matrix, contributing to the formation of a protective barrier. This protective mechanism effectively safeguards the aluminium surface by impeding the penetration of Cl^- ions, thus mitigating the potential degradation. Of particular interest is the AA-40SS composite, which emerges as the embodiment of superior corrosion resistance amongst the reinforced composites. This accomplishment can be attributed to the relatively larger concentration of particulate matter present during the casting process. This characteristic maximizes the amalgamation of particles with the molten metal matrix and diminishes the occurrence of voids within the microstructure [19].

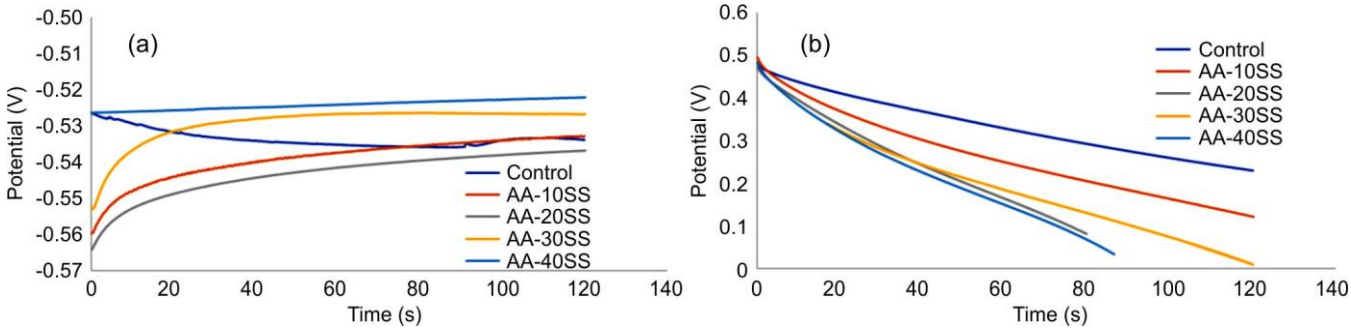

Fig. 2. OCP plots of AA-SS and the control sample in (a) 1 M of HCl and (b) 1 M of NaCl

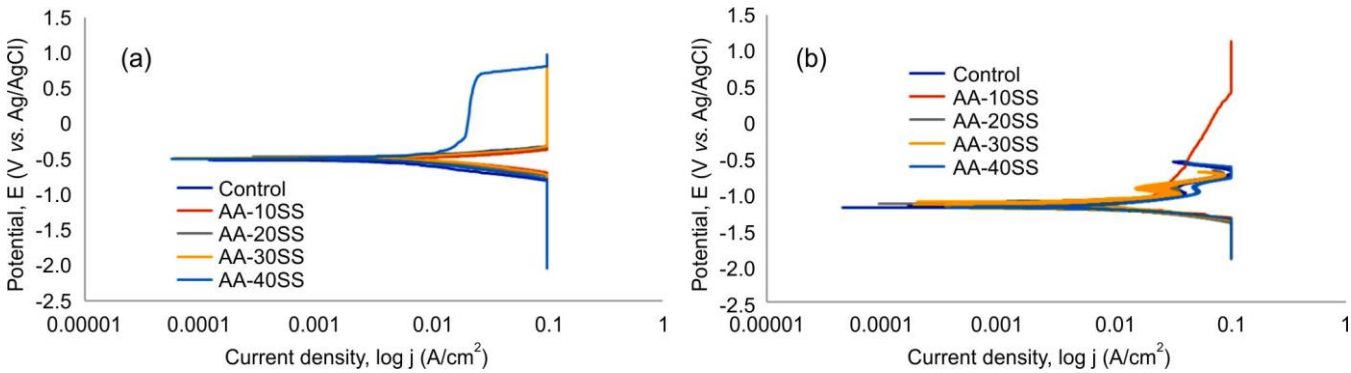

Fig. 3. Polarization plot of the composite in (a) HCl and (b) NaCl

TABLE-3
TAFEL PLOT OF AA-SS COMPOSITES IN HCl

	E_{corr} (V)	J_{corr} (A/cm^2)	CR (mm/yr)	PR (Ω)
Control	-1.49808	0.0775991	32.0701	9.44148
AA-10SS	-1.24630	0.0649111	24.2630	11.40144
AA-20SS	-1.49480	0.0595267	22.6899	13.34460
AA-30SS	-1.87719	0.0556072	11.1095	27.25490
AA-40SS	-1.85140	0.0481750	9.4993	31.54800

Table-4 provides the polarization data and parameters, including corrosion resistance (CR). Furthermore, Fig. 3 displays the polarization data along with the polarization curves essential to AA-SS in the presence of NaCl. Although there is a positive trend as the reinforcement seashells were introduced into the metal matrix, as the CR got improved with each increment in the %wt. composition of SS. AA-10SS had a corrosion rate of 48.8292 mm/yr while AA-40SS had a CR of 26.052 mm/yr. The suitable reaction to corrosion observed in later samples can be attributed to the reinforcement particles. These particles, during the casting process, effectively occupy the voids in the metal structure, significantly hindering the penetration of chloride ions when subjected to a corrosive environment. In Fig. 3b, a shift of the curve towards the positive as the reinforcement contents increase is observed, also there is a deviation in the E_{corr} greater than 0.085 V, which sums up the anodic nature of the seashell reinforcement.

TABLE-4
TAFEL PLOT OF AA-SS COMPOSITES IN NaCl

	E_{corr} (V)	J_{corr} (A/cm^2)	CR (mm/yr)	PR (Ω)
Control	-1.057020	0.0775991	48.8292	9.44148
AA-10SS	-1.111100	0.0649111	44.9602	11.40144
AA-20SS	-1.065320	0.0595267	31.6385	13.34460
AA-30SS	-1.020650	0.0556072	36.6393	27.25490
AA-40SS	-0.902875	0.0481750	26.0520	31.54800

Mechanical studies: Table-5 displays the hardness and the yield strength rating of the matrix material (AA6063) reinforced with particles of seashell (SS). The average hardness (HV) values of the composite samples are higher than that of the control sample. All evidence suggests a consistent increase in the hardness values, which correspond to the increase in weight percentage within the samples (Fig. 4). Clearly, this is demonstrated by the decrease in grain size due to significant nucleation occurring within the coarse eutectic. The improved hardness properties can also be traced to strong interfacial bonding between each intermetallic phase [19]. As illustrated in Fig. 5, the yield strength (YS) increases from 40 MPa in the control sample to a maximum of 130 MPa in the AA-20SS specimen, before decrease to 78 MPa in the AA-40SS specimen. Similarly, the ultimate tensile strength (UTS) increased from 105 MPa in the control sample to 190 MPa in the AA-20SS composite. Among all the composites, AA-20SS appeared to exhibit the highest mechanical performance, absorbing up to 40 J of impact energy. In comparison, AA-30SS and AA-40SS absorbed 35 J and 40 J, respectively. The slightly lower performance of AA-30SS and AA-40SS could

TABLE-5
YIELD STRENGTH COMPOSITES

Samples	Yield strength (MPa)
Control	40
AA-10SS	72
AA-20SS	130
AA-30SS	92
AA-40SS	78

be attributed to uneven distribution of reinforcement along the length of the composites. Although recrystallization is known to inhibit the development of desirable properties [20,21], it is evident that the presence of inherent constituents such as CaO, SiO_2 and Al_2O_3 contributes significantly to the structural refinement and enhances the mechanical behaviour of the aluminum-based alloys.

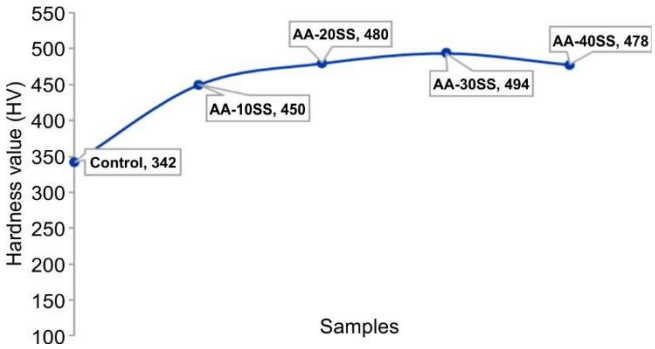

Fig. 4. Hardness value plot of the composite

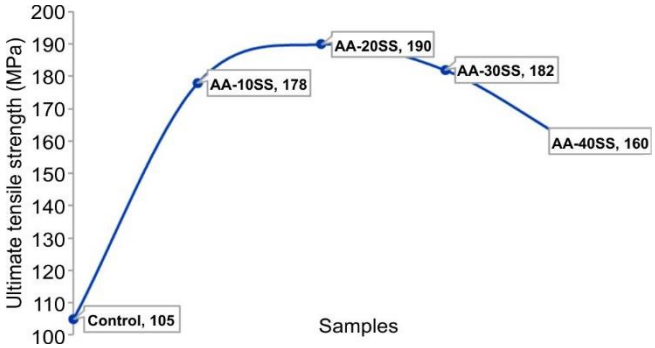

Fig. 5. Ultimate tensile strength of the composites

In Fig. 6, the impact strength behaviour of the composite alloy is examined to determine the optimal response influenced by the weight fraction of the reinforcing particulates. The results indicate that AA-20SS exhibits the highest impact strength, with a slight decline observed in composites with higher reinforcement content. As noted earlier [22,23], supersaturation of whiskers and fibers beyond the optimal threshold can lead to porosity due to excessive crystal growth, even when the reinforcing constituents are inherently present in the alloy matrix. It is also important to observe that defects such as micro-voids, pinholes and pits may form within the ceramic phase as a result of excessive agglomeration, surpassing the ability material to effectively absorb and distribute the reinforcement. The superior performance observed in AA-20SS can be attributed to the moderate and uniform distribution of the metallic phase within the aluminum matrix, ensuring optimal load transfer and impact resistance.

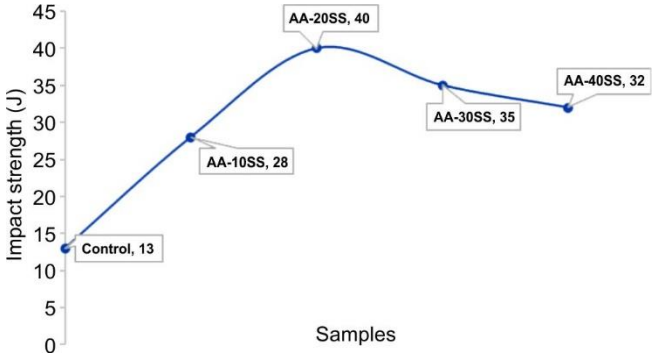

Fig. 6. Impact strength of the composites

Conclusion

In this work, seashells have demonstrated their effectiveness as a reinforcement material, contributing to enhanced anticorrosive performance in the prepared composites. Notably, the AA-40SS sample exhibited a 38.01% improvement in hardness, indicating the strengthening potential of seashell reinforcement. The incorporation of seashells into the AA6063 matrix also led to a significant increase in impact strength, highlighting their role in improving the toughness of the composite. Furthermore, the corrosion analysis revealed reduced deterioration, attributed to the retardation effect of the reinforcement against chloride ion penetration, thereby enhancing the resistance of composite to corrosion.

CONFLICT OF INTEREST

The authors declare that there is no conflict of interests regarding the publication of this article.

REFERENCES

1. O.A. Adetayo and O. Jubril, *FUOYE J. Eng. Technol.*, **4**, 145 (2019); https://doi.org/10.46792/fuoyejet.v4i1.318.
2. I.G. Akande, R.A. Kazeem, T.C. Jen, O.M. Daramola and E.T. Akinlabi, *J. Bio. Tribocorros.*, **10**, 114 (2024); https://doi.org/10.1007/s40735-024-00915-4
3. F. Khan, N. Hossain, J.J. Mim, SM Maksudur Rahman, M.J. Iqbal, M. Billah and M.A. Chowdhury, *J. Eng. Res.*, **13**, 1001 (2025); https://doi.org/10.1016/j.jer.2024.02.017
4. K.O. Babaremu, O.O. Joseph, E.T. Akinlabi, T.C. Jen and O.P. Oladijo, *Heliyon*, **6**, e05506 (2020); https://doi.org/10.1016/j.heliyon.2020.e05506
5. D. Duraibabu, M. Alagar and S.A. Kumar, *RSC Adv.*, **4**, 40132 (2014); https://doi.org/10.1039/C4RA06511E
6. S.P. Dwivedi, P. Sharma and A. Saxena, *Proc. Inst. Mech. Eng., E J. Process Mech. Eng.*, **234**, 543 (2020); https://doi.org/10.1177/0954408920930634
7. F.O. Edoziuno, C.C. Nwaeju, A.A. Adediran, B.U. Odoni and V.R. Arun Prakash, *Sci. Afr.*, **12**, e00781 (2021); https://doi.org/10.1016/j.sciaf.2021.e00781
8. O.S.I. Fayomi, J.W. Sojobi, M.O. Nkiko, I.G. Akande and A.A. Noiki, *AIP Conf. Proc.*, **2437**, 020123 (2022); https://doi.org/10.1063/5.0093172
9. O.S. Fayomi and J.O. Atiba, *Results Surf. Interfaces*, **17**, 100314 (2024); https://doi.org/10.1016/j.rsurfi.2024.100314
10. O.S. Fayomi, *Hybrid Advances*, **6**, 100247 (2024); https://doi.org/10.1016/j.hybadv.2024.100247
11. M. Ferry and P.R. Munroe, *Mater. Sci. Eng. A*, **358**, 142 (2003); https://doi.org/10.1016/S0921-5093(03)00333-2
12. S.K. Gaurav, V.K. Singh and S. Chauhan, *J. Mater. Environ. Sci.*, **15**, 1526 (2024).
13. O. Guillon, J. GonzalezJulian, B. Dargatz, T. Kessel, G. Schierning, J. Räthel and M. Herrmann, *Adv. Eng. Mater.*, **16**, 830 (2014); https://doi.org/10.1002/adem.201300409
14. Z.-Y. Hu, Z.-H. Zhang, X.-W. Cheng, F.-C. Wang, Y.-F. Zhang and S.-L. Li, *Mater. Des.*, **191**, 108662 (2020); https://doi.org/10.1016/j.matdes.2020.108662
15. A. Islam, S.P. Dwivedi, R. Yadav and V.K. Dwivedi, *J. Inst. Eng. India: Series D*, **102**, 317 (2021); https://doi.org/10.1007/s40033-021-00292-z
16. A.J. Knowles, X. Jiang, M. Galano and F. Audebert, *J. Alloys Compd.*, **615**, S401 (2014); https://doi.org/10.1016/j.jallcom.2014.01.134
17. N.C. Okonkwo and I.U. Abdullahi, *Multidiscipl. J. Eng.*, **11**, 15 (2023).
18. B. Parveez, M.A. Maleque and N.A. Jamal, *J. Mater. Sci.*, **56**, 16195 (2021); https://doi.org/10.1007/s10853-021-06305-2
19. J. Garg, M.N. Chiu, S. Krishnan, R. Kumar, M. Rifah, P. Ahlawat, N.K. Jha, K.K. Kesari, J. Ruokolainen and P.K. Gupta, *Appl. Biochem. Biotechnol.*, **196**, 1043 (2024): https://doi.org/10.1007/s12010-023-04570-2
20. S.N.A. Safri, M.T.H. Sultan, M. Jawaid and K. Jayakrishna, *Compos., Part B Eng.*, **133**, 112 (2018); https://doi.org/10.1016/j.compositesb.2017.09.008
21. O. Sanni, J. Ren and T.C. Jen, *Results Eng.*, **16**, 100676 (2022); https://doi.org/10.1016/j.rineng.2022.100676
22. Q. Tan, J. Zhang, Q. Sun, Z. Fan, G. Li, Y. Yin, Y. Liu and M.X. Zhang, *Acta Mater.*, **196**, 1 (2020); https://doi.org/10.1016/j.actamat.2020.06.026
23. X. Zhang, Q. Zhou, K. Wang, Y. Peng, J. Ding, J. Kong and S. Williams, *Mater. Des.*, **166**, 107611 (2019); https://doi.org/10.1016/j.matdes.2019.107611